

## Realization of Four-Level Qudits Using Biphotons

E. V. Moreva\*

*Moscow Engineering Physics Institute, State University, Russia*

G. A. Maslennikov

*National University of Singapore, Singapore*

S. S. Straupe and S. P. Kulik

*Faculty of Physics, Moscow State University, Russia*

(Received 13 January 2006; published 13 July 2006)

The novel experimental realization of four-level optical quantum systems (ququarts) is presented. We exploit the polarization properties of the frequency nondegenerate biphoton field to obtain such systems. A simple method that does not rely on an interferometer is used to generate and measure the sequence of states that can be used in quantum key distribution protocol.

DOI: [10.1103/PhysRevLett.97.023602](https://doi.org/10.1103/PhysRevLett.97.023602)

PACS numbers: 42.50.Dv, 03.67.Mn

*I. Introduction.*—Recently multidimensional ( $D > 2$ ) quantum systems or qudits have attracted a lot of attention in the context of quantum information and communication. It is partly caused by fundamental aspects of quantum theory since the usage of qudits allows one to violate Bell-type inequalities longer than with two dimensional systems (for the references see the review in Ref. [1]). Much of the interest in qudits also comes from the application point of view, especially from the applied quantum key distribution (QKD). Multilevel systems are proved to be more robust against noise in the transmission channel, although measurement and preparation procedures of such systems seems to be much more technically complicated than in the case of qubits. Different aspects of the security of qudit-based protocols have been analyzed [2,3]. Lately a proof-of-principle realization of a QKD protocol with entangled qutrits ( $D = 3$ ) [4] and with qudits [5] has been demonstrated. Over the past few years several elegant experiments have been performed where different kinds of optical qudits were introduced [5–12]. Recently an experiment that ensured the full control over a polarization qutrit state was demonstrated [12,13]. However, polarization qutrits do not seem to serve as a practical candidate for the multilevel QKD, since it is impossible to achieve a demanded state using only SU2 transformations that are done with linear optical elements.

In this Letter we present the results of the experimental preparation, transformation, and measurement carried out with polarization-based ququarts or quantum systems with dimensionality  $D = 4$ .

*II. Polarization ququarts and their properties.*—If one considers the two-photon field, generated via the spontaneous parametric down-conversion (SPDC) process, then the pure polarization state can be written as a superposition of four basic components:

$$|\Psi\rangle = c_1|H_1, H_2\rangle + c_2|H_1, V_2\rangle + c_3|V_1, H_2\rangle + c_4|V_1, V_2\rangle. \quad (1)$$

Here  $c_i = |c_i|e^{i\phi_i}$ , ( $i = 1, 2, 3, 4$ ) are complex probability amplitudes,  $|H_j\rangle \equiv a_{\lambda_j}^\dagger|\text{vac}\rangle$ ,  $|V_j\rangle \equiv b_{\lambda_j}^\dagger|\text{vac}\rangle$ , where  $\lambda_j$ , ( $j = 1, 2$ ) are the central wavelengths of down-converted photons. If the down-converted photons have only a polarization degree of freedom, then a ququart state (1) converts to a qutrit state; i.e., middle terms in (1) become indistinguishable. In order to distinguish between these terms one must be able to distinguish between the down-converted photons either in frequency, momentum, or detection time. In experiments, described in this Letter, we chose the collinear nondegenerate regime of SPDC, so twin photons that form a biphoton were having different frequencies and propagating simultaneously along the same direction. The sum of their frequencies was equal to the frequency of the pump, according to energy conservation. Polarization properties of this state can be described by Stokes parameters, which are defined as the mean values of Stokes operators, averaged over a state (1):

$$\begin{aligned} \langle S_0 \rangle &= \langle a_1^\dagger a_1 + a_2^\dagger a_2 + b_1^\dagger b_1 + b_2^\dagger b_2 \rangle = 2; \\ \langle S_1 \rangle &= \langle a_1^\dagger a_1 + a_2^\dagger a_2 - b_1^\dagger b_1 - b_2^\dagger b_2 \rangle \\ &= 2(|c_1|^2 - |c_4|^2); \\ \langle S_2 \rangle &= \langle a_1^\dagger b_1 + a_2^\dagger b_2 + b_1^\dagger a_1 + b_2^\dagger a_2 \rangle \\ &= 2\text{Re}(c_1^*(c_2 + c_3) + c_4(c_2^* + c_3^*)); \\ \langle S_3 \rangle &= \langle a_1^\dagger b_1 + a_2^\dagger b_2 - b_1^\dagger a_1 - b_2^\dagger a_2 \rangle \\ &= 2\text{Im}(c_1^*(c_2 + c_3) + c_4(c_2^* + c_3^*)). \end{aligned} \quad (2)$$

Although the description of the light polarization can be introduced only for the quasimonochromatic plane waves, it is possible to use  $P$ -quasispin formalism [14] to describe the polarization of arbitrary quantum beams with  $n$  modes, frequency or spatial. It is worth noting that the frequency representation of the ququart (1) is isomorphic to the spatial one, when twin photons have the same frequencies but propagate in different directions [15]. Frequently in the

tasks of quantum communication it is convenient to operate with states in a single-spatial mode. For the two-frequency and single-spatial mode field, the formal definition of annihilation or creation operators is given by the sum of corresponding operators in each mode. Also we take into account that these operators do commute for different frequency modes. So the Stokes parameters will contain time dependent terms  $\exp(i(\omega_1 - \omega_2)t)$  that describe “beats” of frequency modes and have no connection with the light polarization. However, these terms vanish if one considers the finite detection time, which allows one to classically average these beats.

The polarization degree is given by

$$P_4 = \frac{\sqrt{\sum_{k=1}^3 \langle S_k^{(1)} + S_k^{(2)} \rangle^2}}{\langle S_0^{(1)} + S_0^{(2)} \rangle}. \quad (3)$$

This definition of the polarization degree is just generalization of the commonly used classical one. It differs from the definition suggested in Ref. [16], where it serves as a witness of the state purity. In the case of polarization-based qutrit states [12,13], the polarization degree  $P_3 = \sqrt{|c'_1|^2 - |c'_3|^2 + 2|c'_1 c'_2 + c'_2 c'_3|^2}$  with  $c'_1 = c_1$ ,  $\sqrt{2}c'_2 = c_2 = c_3$ ,  $c'_3 = c_4$  in (1) was an invariant to unitary polarization transformations. Indeed it is impossible to prepare all demanded pure states, unless one uses interferometric schemes with several nonlinear crystals [12]. In particular, there is no way to transform the basic qutrit state  $|\Psi'_4\rangle = |V, V\rangle$  with  $P = 1$  into the state  $|\Psi'_2\rangle = |H, V\rangle$  with  $P = 0$  using retardation plates. However, in the case of polarization ququarts, this quantity is no longer the invariant and can be changed by applying local unitary transformations in each frequency mode. It can be achieved by using dichroic polarization transformers, which act separately on the photons with different frequencies. For example, to transform the state  $|\Psi_4\rangle = |V_{\lambda_1}, V_{\lambda_2}\rangle$  into the state  $|\Psi_2\rangle = |H_{\lambda_1}, V_{\lambda_2}\rangle$  one needs to use the retardation plate which serves as a half wave plate at  $\lambda_1$  and as a wave plate at  $\lambda_2$ . The unitary transformation on the state (1) is given by  $4 \times 4$  matrix that is obtained by a direct product of two  $2 \times 2$  matrices describing the transformation performed on each photon:

$$G \equiv \begin{pmatrix} t_1 t_2 & t_1 r_2 & r_1 t_2 & r_1 r_2 \\ -t_1 r_2^* & t_1 t_2^* & -r_1 r_2^* & r_1 t_2^* \\ -r_1^* t_2 & -r_1^* r_2 & t_1^* t_2 & t_1^* r_2 \\ r_1^* r_2^* & -r_1^* t_2^* & -t_1^* r_2^* & t_1^* t_2^* \end{pmatrix}, \quad (4)$$

with “transmission” and “reflection” coefficients  $t_i = \cos \delta_i + i \sin \delta_i \cos 2\alpha_i$ ,  $r_i = i \sin \delta_i \sin 2\alpha_i$ ,  $\delta_i = \pi(n_o - n_e)h/\lambda_i$ , where  $\delta_i$  is its optical thickness,  $h$  is the geometrical thickness, and  $\alpha_i$  is the orientation angle between the optical axis of a wave plate and vertical direction. So for the unitary transformation of the ququart the nonzero elements of the matrix considered above are

$$G_{13} = G_{24} = G_{31} = G_{42} = 1. \quad (5)$$

The same dichroic plate performs direct and reverse unitary transformations between the polarization Bell states:  $|\Phi^{+(-)}\rangle$  and  $|\Psi^{+(-)}\rangle$ , which are represented by ququarts with  $c_2 = c_3 = 0$ ,  $c_1 = +(-)c_4 = \frac{1}{\sqrt{2}}$  and  $c_1 = c_4 = 0$ ,  $c_2 = +(-)c_3 = \frac{1}{\sqrt{2}}$  correspondingly. Similar transformations with frequency nondegenerate biphotons have been realized in Ref. [17].

In general, to prepare an arbitrary ququart state (1) it is necessary to use four nonlinear crystals arranged in such a way that each crystal emits coherently one basic state in the same direction. But in particular cases a reduced set of crystals is quite sufficient to generate specific ququart states which can be used in applications. For example, to prepare the polarization Bell states it was sufficient to use two crystals [17,18]. Moreover, even single crystal allows one to prepare the useful subset of ququarts.

*III. Polarization ququarts in QKD protocol.*—The complete QKD protocol with four-dimensional polarization states exploits five mutually unbiased bases with four states in each. In terms of biphoton states the first three bases consist of product polarization states of two photons while the last two bases consist of two-photon entangled states:

$$\begin{aligned} (I) & |H_1 H_2\rangle; & |H_1 V_2\rangle; & |V_1 H_2\rangle; & |V_1 V_2\rangle, \\ (II) & |D_1 D_2\rangle; & |D_1 A_2\rangle; & |A_1 D_2\rangle; & |A_1 A_2\rangle, \\ (III) & |R_1 R_2\rangle; & |R_1 L_2\rangle; & |L_1 R_2\rangle; & |L_1 L_2\rangle, \\ (IV) & |R_1 H_2\rangle + |L_1 V_2\rangle; & |R_1 H_2\rangle - |L_1 V_2\rangle; & & (6) \\ & |L_1 H_2\rangle + |R_1 V_2\rangle; & |L_1 H_2\rangle - |R_1 V_2\rangle, \\ (V) & |H_1 R_2\rangle + |V_1 L_2\rangle; & |H_1 R_2\rangle - |V_1 L_2\rangle; & & \\ & |H_1 L_2\rangle + |V_1 R_2\rangle; & |H_1 L_2\rangle - |V_1 R_2\rangle. \end{aligned}$$

Here  $H, V, D, A, R, L$  indicate horizontal, vertical, +45 and -45 linear, right- and left-circular polarization modes, respectively, and lower indices numerate the frequency modes of two photons. It has been proved [3] that using only first two or three bases is sufficient for the efficient QKD. Exploiting the incomplete set of bases one sacrifices the security but enhances the key generation rate. That is why we will restrict ourselves to the first three bases and skip the rest two. As we will show experimentally, the set of 12 states can be prepared with a single nonlinear crystal and local unitary transformations. We also present a measurement scheme that allows one to discriminate the states belonging to one basis deterministically.

*IV. Experiment.*—

*A. Experimental setup.*—The experimental setup for generation and measurement of ququart states is shown at Fig. 1. The 10 mW cw He-Cd laser operating at 325 nm serves as a pump. A 15 mm lithium-iodate type I crystal emits down-converted photons at central wavelengths  $\lambda_1 = 702$  nm,  $\lambda_2 = 605$  nm within the spectral width of 2 nm each, propagating collinearly with the pump, so the

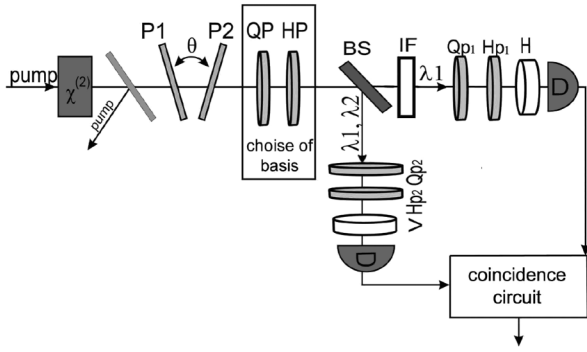


FIG. 1. Setup for preparation and measurement of ququarts.

ququart state  $|V_1V_2\rangle$  is generated. Then, this state was subjected to transformations done by dichroic wave plate(s). Finally the state passed through the zero-order half and quarter plates depending on which bases has been chosen. The measurement setup consists of a Brown-Twiss scheme with a nonpolarizing beam splitter. An interference filter centered at 702 nm with a FWHM bandwidth of 3 nm was placed in transmitted arm. This part of the scheme allows one to reconstruct arbitrary polarization biphoton-ququart by registering coincidence counts for different projections that are done by the polarization filters located in each arm [19]. Each filter consists of a zero-order quarter and half wave plate and a fixed analyzer. Two Si avalanche photo-diodes, linked to a coincidence scheme with 1.5 nsec time window, were used as single-photon detectors.

**B. Experimental procedure.**—Let us consider as an example, the preparation of a state  $|H_1V_2\rangle$  from the initial state  $|V_1V_2\rangle$ . This transformation can be achieved by a dichroic wave plate oriented at  $45^\circ$  that introduces a phase shift of  $2\pi$  between extra and ordinary polarized photons at 605 nm, and a phase shift of  $\pi$  for the conjugate photons at 702 nm. Using quartz as birefringent material it is easy to calculate that the one of the possible thicknesses of the wave plate that does this transformation should be equal to 3.406 mm [20]. We used two plates P1 and P2 with an effective thickness of 3.401 mm. If then one can tilt these wave plates toward each other by a finite angle  $\theta$ , then the optical thickness of the effective wave plate will be changing and, at a certain value of  $\theta$ , the desired transformation will be achieved. This corresponds to maximal coincidence rate when the measurement part is tuned to select  $|H_1V_2\rangle$  state. Monitoring the coincidences, one can obtain the value of  $\theta$  for which the main maximum occurs. Then, fixing the tilting angle at this value, one can perform a complete quantum state tomography protocol in order to verify if the state really coincides with the ideal. In order to change the basis from *I* to *II* (*III*), zero-order half (quarter) wave plates oriented at  $22.5^\circ$  ( $45^\circ$ ) were used.

**V. Results and discussion.**—Figure 2 shows the coincidences and single count rates versus the tilting angle  $\theta$  which determines optical thickness of the effective wave plate. If the measurement setup is tuned to select the state  $|H_1V_2\rangle$  then dependence of coincidences rate on the plate

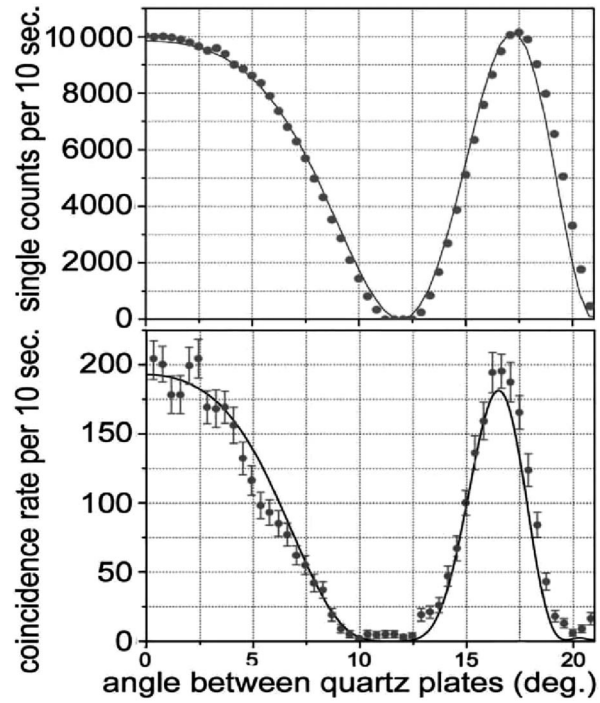


FIG. 2. Dependence of single counts (upper) and coincidences (lower) on tilting angle  $\theta$ .

optical thicknesses  $\delta_i$  is given by formula:

$$R_{\text{coin}} \propto \langle a_1^\dagger b_2^\dagger a_1 b_2 \rangle = \sin^2(\delta_1)\cos^2(\delta_2), \quad (7)$$

whereas the single counts rate in the upper channel is

$$I_{702 \text{ nm}} \propto \langle a_1^\dagger a_1 \rangle = \sin^2(\delta_1). \quad (8)$$

The solid lines in Fig. 2 show the theoretical curves. We performed tomography measurements for the main and additional maxima as well as for the minimum. The minima in coincidences occur when intensity in any channel drops to zero, so it is not a necessary condition for distinguishing the orthogonal state to the one selected by given settings of polarization filters. Nevertheless, according to

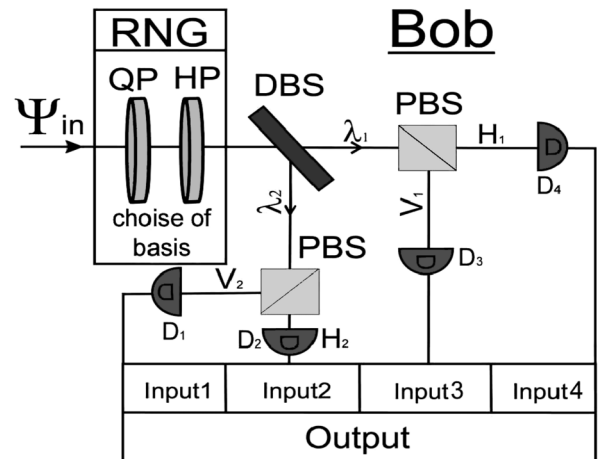


FIG. 3. Measurement part at Bob's station.

TABLE I. Density matrix components and fidelities for selected transformations.

State	$\rho_{11}^{\text{exp}}(\rho_{11}^{\text{th}})$	$\rho_{22}^{\text{exp}}(\rho_{22}^{\text{th}})$	$\rho_{33}^{\text{exp}}(\rho_{33}^{\text{th}})$	$\rho_{44}^{\text{exp}}(\rho_{44}^{\text{th}})$	$F$
$ H_1V_2\rangle$	0(0)	0.984(1)	0(0)	0.016(0)	0.98
$ V_1H_2\rangle$	0.024(0)	0.004(0)	0.944(1)	0.028(0)	0.94
$ D_1A_2\rangle$	0(0)	0.994(1)	0(0)	0.006(0)	0.99
$ A_1D_2\rangle$	0.015(0)	0(0)	0.950(1)	0.035(0)	0.95
$ R_1L_2\rangle$	0(0)	0.973(1)	0.027(0)	0(0)	0.97
$ L_1R_2\rangle$	0.016(0)	0(0)	0.957(1)	0.027(0)	0.96

calculations and our measurements the minimum in the coincidences at Fig. 2 exactly refers to the state  $|V_1H_2\rangle$ . Starting from the  $|V_{702\text{ nm}}V_{605\text{ nm}}\rangle$  we prepared and measured the whole set of the states from (6) belonging to the first three bases. Table I shows components of the experimental (theoretical) density matrix as well as fidelity  $F$  defined by  $F = \text{Tr}(\rho_{\text{th}}\rho_{\text{exp}})$  for some of the states.

The method discussed in this Letter allows one to unambiguously distinguish all states forming chosen bases. The measurement setup which has been already tested in our experiments is shown on the Fig. 3. It consists of the dichroic mirror, separating the photons with the different wavelengths, and a pair of polarization beam splitters, separating photons with orthogonal polarizations. We would like to stress that using dichroic beam splitter allows one to achieve 100% mode separation efficiency which is not possible for qutrits. The four-input double-coincidence scheme linked to the outputs of single-photon detectors registers the biphotons-ququarts. For example for the basis I, the scheme works as follows: (i) if state  $|H_1H_2\rangle$  comes, then detectors D4, D2 will fire, (ii) if state  $|H_1V_2\rangle$  comes, then detectors D4, D1 will fire, (iii) if state  $|V_1H_2\rangle$  comes, then detectors D3, D2 will fire, (iv) if state  $|V_1V_2\rangle$  comes, then detectors D3, D1 will fire. The same holds for any of the remaining correctly guessed bases, since the quarter and half wave plates transform the polarization to an  $HV$  basis in which the measurement is performed. The registered coincidence count from a certain pair of detectors contributes to the corresponding diagonal component of the measured density matrix. If the basis is guessed correctly, then the registered coincidence count deterministically identifies the input state. We illustrate this statement by Table II, which shows total number of registered events per 30 sec for the input state  $|R_1L_2\rangle$  measured in circular basis and calculated components of the experimental (theoretical) density matrix.

To conclude, we have suggested and tested a novel method of the preparation, and measurement of the subset of four-dimensional polarization quantum states. Since for this class of states the polarization degree is not invariant under SU2 transformations it is possible to switch between states using simple polarization elements.

TABLE II. Coincidence rate and density matrix components.

$D_4D_2$	$\rho_{11}$	$D_4D_1$	$\rho_{22}$	$D_3D_2$	$\rho_{33}$	$D_3D_1$	$\rho_{44}$
0	0.0(0)	220	0.973(1)	6	0.027(0)	0	0.0(0)

This work was supported in part by Russian Foundation of Basic Research No. 06-02-16769, MSU interdisciplinary grant, and Russian Agency of Science and Innovations No. 2006-RI-19.0/001/593.

\*Electronic address: ekaterina.moreva@gmail.com

- [1] M. Genovese, Phys. Rep. **413**, 319 (2005).
- [2] H. Bechmann-Pasquinucci and A. Peres, Phys. Rev. Lett. **85**, 3313 (2000); D. Bruß and C. Macchiavello, Phys. Rev. Lett. **88**, 127901 (2002); V. Karimipour and A. Bahraminasab, Phys. Rev. A **65**, 052331 (2002); M. Bourennaneet *et al.*, J. Phys. A **35**, 10 065 (2002); M. Genovese and C. Novero, Eur. Phys. J. D **21**, 109 (2002).
- [3] H. Bechmann-Pasquinucci and W. Tittel, Phys. Rev. A **61**, 062308 (2000); M. Bourennane, A. Karlsson, and G. Björk, Phys. Rev. A **64**, 012306 (2001); N. Cerf *et al.*, Phys. Rev. Lett. **88**, 127902 (2002); F. Caruso, H. Bechmann-Pasquinucci, and C. Macchiavello, Phys. Rev. A **72**, 032340 (2005).
- [4] S. Gröblacher *et al.*, New J. Phys. **8** 75 (2006); G. Molina-Terriza *et al.*, Phys. Rev. Lett. **92**, 167903 (2004).
- [5] S. Walborn *et al.*, Phys. Rev. Lett. **96**, 090501 (2006).
- [6] M. O'Sullivan-Hale *et al.*, Phys. Rev. Lett. **94**, 220501 (2005); L. Neves *et al.*, Phys. Rev. Lett. **94**, 100501 (2005).
- [7] A. Vaziri, G. Weihs, and A. Zeilinger, Phys. Rev. Lett. **89**, 240401 (2002); N. Langford *et al.*, Phys. Rev. Lett. **93**, 053601 (2004).
- [8] R. T. Thew *et al.*, Quantum Inf. Comput. **4**, 93 (2004).
- [9] R. T. Thew *et al.*, Phys. Rev. Lett. **93**, 010503 (2004).
- [10] H. de Riedmatten *et al.*, Phys. Rev. A **69**, 050304 (2004); D. Stucki, H. Zbinden, and N. Gisin, quant-ph/0502169.
- [11] J.C. Howell, A. Lamas-Linares, and D. Bouwmeester, Phys. Rev. Lett. **88**, 030401 (2002).
- [12] Yu. Bogdanov *et al.*, Phys. Rev. Lett. **93**, 230503 (2004).
- [13] Yu. Bogdanov *et al.*, Phys. Rev. A **70**, 042303 (2004).
- [14] V.P. Karassiov, J. Phys. A **26**, 4345 (1993).
- [15] D.F.V. James *et al.*, Phys. Rev. A **64**, 052312 (2001).
- [16] A. Sehat *et al.*, Phys. Rev. A **71**, 033818 (2005).
- [17] A.V. Burlakov *et al.*, JETP **95**, 639 (2002).
- [18] Y.H. Kim, S.P. Kulik, and Y. Shih, Phys. Rev. A **63**, 060301 (2001).
- [19] Yu. I. Bogdanov *et al.*, JETP Lett. **82**, 164 (2005).
- [20] The thickness of the retardation plate that performs the transformation is determined by the number of order  $m_i$  that is chosen for the specified wavelength according to  $\frac{m_2\lambda_2}{\delta n_2} = \frac{(2m_1+1)\lambda_1}{2\delta n_1}$ . Here  $\delta n_i$  is the value of the birefringence for the specific wavelength. We chose order  $m_1 = 51$  for  $\lambda = 702\text{ nm}$  and  $m_2 = 47$  for  $\lambda = 650\text{ nm}$ .